ADAPTIVE CHIRPLET BASED SIGNAL APPROXIMATION

Shie Qian, Dapang Chen
DSP Group, National Instruments,
6504 Bridge Point Parkway, Austin, TX 78730, USA

Qinye Yin
Information and Control Department
Xi'an Jiaotong University, Xi'an, P.R. China

ABSTRACT

The chirp function is one of the most fundamental functions in nature. Many natural events can be roughly approximated by a group of chirp functions. In this paper, we present a practical adaptive chirplet based signal approximation algorithm. Unlike the other chirplet decompositions known so far, the elementary chirplet functions employed in this algorithm are adaptive. Therefore, the resulting approximation could better match the underlying signal and uses fewer coefficients. The effectiveness of the algorithm is demonstrated by numerical simulations.

1. INTRODUCTION

It is well understood that the chirp is one of the most important functions in nature. Many natural phenomena, for instance, the impulsive signal that is dispersed by the ionosphere [6], the bird sound, and the human voice, could roughly be approximated by a group of chirp functions. If the chirp function has a smooth amplitude, such as that of a Gaussian envelope, then it becomes a typical AM-FM model, e.g.,

$$h_p(t) = \left(\frac{\alpha_p}{\pi}\right)^{1/4} e^{-\alpha_p(t-t_p)^2/2 + j(\omega_p t + \beta_p t^2/2)} \qquad \alpha_p \geq 0 \tag{1}$$

Because $h_p(t)$ in Eq.(1) only lasts for a short time period, it is named *chirplet* in some literature ([1] and [3]). It is interesting that the chirplet is the only function whose *Wigner-Ville distribution* is non-negative. Therefore, the chirplet also plays an important role in the area of joint time-frequency analysis.

Since the chirplet is fundamental, it is desirable to have a method of representing a signal in terms of weighted chirplets. In [1] and [3], the parameters (α_p, t_p, ω_p, β_p) of the chirplet $h_p(t)$ are limited to a fixed grid. They are easier to implement, but do not always fit the underlying signal well. The adaptive method [4] (also known as the *matching pursuit* [5]) is presumably able to better characterize the signal's nature, but its implementation is much more involved. So far, no practical chirplet based matching pursuit algorithm has been reported.

It is the goal of this paper to introduce a feasible algorithm to represent an arbitrary signal in terms of group adaptive chirplets. The paper is arranged as follows. First, we briefly review the general matching pursuit scheme. The bottleneck in realizing the matching pursuit is estimating the optimal chirplet. In section 3, we will give a detailed treatment of computing optimal chirplets. Finally, a few numerical examples are presented to demonstrate the effectiveness of the algorithm introduced in this paper.

2. ADAPTIVE APPROXIMATION

For a signal $s(t)$, we could have a following representation,

$$s(t) = \sum_{p=0}^{P-1} A_p h_p(t) + s_{p+1}(t) \tag{2}$$

where $s_{p+1}(t)$ denotes the difference between $s_p(t)$ and $A_p h_p(t)$, i.e.,

$$s_{p+1}(t) = s_p(t) - A_p h_p(t) \tag{3}$$

Note that $s_0(t) = s(t)$. The coefficient A_p is the regular inner product between the signal $s_p(t)$ and the adaptive function $h_p(t)$, i.e.,

$$A_p = \int s_p(t) h_p(t) dt \tag{4}$$

The adaptive elementary function $h_p(t)$ is chosen such that the residual $\|s_{p+1}(t)\|^2$ is minimum, i.e.,

$$min_{h_p} \|s_{p+1}(t)\|^2 = min_{h_p} \|s_p(t) - A_p h_p(t)\|^2 \tag{5}$$

which is equivalent to

$$max_{h_p}|A_p|^2 = max_{h_p}\left|\int s_p(t)h_p(t)dt\right|^2 \tag{6}$$

It can be proved [7] that the residual $\|s_{p+1}(t)\|^2$ monotonically decreases as P, the number of terms, increases. When P is large enough and the number of samples is finite, the residual may reduce to zero!

The approximation scheme described by Eq.(2) to (6) is called the *matching pursuit* in some literature. It was independently developed by the authors ([4] and [5]) and Mallat and Zhang [2] around the same time period.

The key step of the matching pursuit is to solve the optimization problem posted in Eq.(6). In principle, the convergence of the residual $\|s_{p+1}(t)\|^2$ is independent of the type of elementary functions $h_p(t)$ used. In other words, any function can be used to match the underlying signal. For a practical implementation, however, we have to limit $h_p(t)$ to certain simple parametric models. Otherwise, it will be too complicated to solve Eq.(6). Previously, $h_p(t)$ was limited to be the frequency modulated Gaussian function, that is, $\beta_p = 0$ in Eq.(1).

Because of the limitation of the frequency modulated Gaussian elementary functions, researchers have proposed the chirplet based adaptive approximation method. So far, however, no practical implementation has been reported. The main difficulty lies in the solution of Eq.(6) when $h_p(t)$ is a four-parameter chirplet. In the next section, we will address this problem.

3. ESTIMATION OF OPTIMAL CHIRPLETS

Applying the zooming principle, we developed the so-called *zooming algorithm* to estimate the optimal chirplet with $\beta_p = 0$ (frequency modulated Gaussian elementary function). In what follows, we shall list some important results without justification. The reader can find a comprehensive treatment of the zooming algorithm in [5] and [7].

The outputs of the zooming algorithm are:

- the time variance $1/d$, where $d \geq \alpha_p$. The equality holds for $\beta_p = 0$;
- the center time $\langle t \rangle$, where $\langle t \rangle = t_p$;
- the mean frequency $\langle \omega \rangle$. $\langle \omega \rangle = \omega_p$, for $\beta_p = 0$.

By using the zooming algorithm, we can completely determine the optimal $h_p(t)$ in Eq.(1) for $\beta_p = 0$. Unfortunately, it is not the case when $h_p(t)$ is a general chirplet function.

The zooming algorithm introduced in [5] essentially only uses the time waveform. As a matter of fact, the power spectrum of $h_p(t)$ also contains useful information as illustrated in Figure 1.

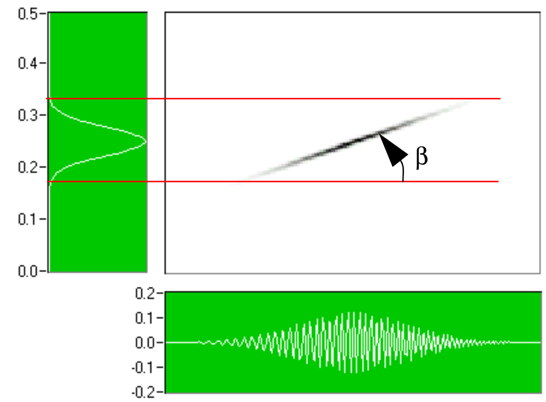

Figure 1 The width of the power spectrum is proportional to the frequency change rate β.

The bottom plot of Figure 1 illustrates a typical chirplet defined in Eq.(1). The left plot depicts the corresponding power spectrum. The middle one is the *Wigner-Ville distribution* given by

$$WVD_p(t, \omega) = 2e^{-\alpha_p(t-t_p)^2 - (\omega - \omega_p - \beta_p t)^2/\alpha_p} \tag{7}$$

which is non-negative. As shown in Figure 1, the width of the power spectrum of $h_p(t)$ is proportional to the frequency change rate $|\beta_p|$. The larger the $|\beta_p|$, the wider the width of the power spectrum. Applying the Wigner-Ville distribution's marginal property [7], we can compute the analytical form of the power spectrum of $h_p(t)$, i.e.,

$$|H_p(\omega)|^2 = \int WVD_p(t, \omega)dt = 2\sqrt{\frac{\pi}{c}}e^{-(\omega - \omega_p - \beta_p t_p)^2/c} \tag{8}$$

which is a Gaussian function with the mean frequency

$$\langle \omega \rangle = \omega_p + \beta_p t_p \tag{9}$$

Note that the quantity $\langle\omega\rangle$ is estimated by the zooming algorithm. When $\beta_p = 0$, $\langle\omega\rangle = \omega_p$.

The variance of the power spectrum of $h_p(t)$ in Eq.(8) is

$$c = \frac{\alpha_p^2 + \beta_p^2}{\alpha_p} \tag{10}$$

which implies that α_p is strictly less than c. When $\beta_p = 0$, $c = \alpha_p = d$, where $1/d$ is the time variance estimated by the zooming algorithm.

Now, the estimation procedure can be summarized as follows:

1. Apply the zooming algorithm to estimate the time variance $1/d$, center time $<t>$ (that is equal to t_p), and mean frequency $<\omega>$;
2. Compute the signal's power spectrum;
3. In the frequency domain, estimate the frequency variance c of the Gaussian function centered at $<\omega>$;
4. Check if $c = d$. If so, then $\beta_p = 0$. In this case, $\alpha_p = d = c$, $t_p = <t>$, $\omega_p = <\omega>$. Otherwise, go to the next step;
5. Set the initial value of α_p to d;
6. Compute β_p via Eq.(10) and then ω_p via Eq.(9);
7. Construct $h_p(t)$ in Eq.(1);
8. Compute the inner product of $h_p(t)$ and $s_p(t)$ in Eq.(4);
9. Reduce α_p by a small quantity Δ, that is, $\alpha_p =: \alpha_p - \Delta$. Then, repeat Step 6. to Step 8. until $\alpha_p = 0$. The parameters $(\alpha_p, t_p, \omega_p, \beta_p)$ corresponding to the largest $|A_p|^2$ constitute the optimal chirplet $h_p(t)$.

The most time consuming task is Step 9. The decrement Δ balances the processing time and the estimation accuracy. Obviously, the bigger the Δ, the poorer the accuracy (but less time). Because $|A_p|^2$ is less sensitive to small α_p, instead of using a uniform decrement Δ, we start with a small Δ and then gradually increase it as α_p gets smaller. By doing so, we could substantially improve the processing speed without scarifying the accuracy.

4. NUMERICAL SIMULATIONS

The test signal used in this section is an echo-location pulse emitted by a large brown bat, *Eptesicus fuscus*. The original data, as shown in Figure 2, contains 400 samples. Table 1 lists the number of chirplets used and corresponding residual and the processing time based on the Micron Pentium 120 PC with 32M RAM. The relative residual there is defined by

$$residual = \frac{\|s_P(t)\|^2}{\|s(t)\|^2} \times 100 \tag{11}$$

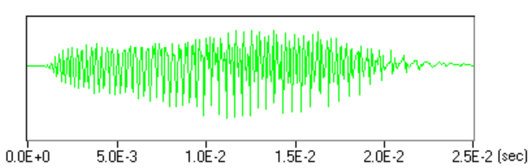

Figure 2 Bat Sound (Bat data provided by Curtis Condon, Ken White, and Al Feng of the Beckman Institute at the University of Illinois.)

Note that each chirplet is completely determined by four parameters $(\alpha_p, t_p, \omega_p, \beta_p)$ plus a coefficient A_p. As shown in Table 1, by using five chirplets (that is, 25 parameters) we could represent 400-sample bat sound with a residual less than ten percent. The computation time required is less than half a second.

Table 1:

Number of Chirplets	Residual (%)	Processing Time (second)
1	58.0	0.11
2	31.1	0.22
3	22.7	0.29
4	15.9	0.38
5	9.76	0.49

Figure 3 to Figure 7 illustrate time-dependent spectra computed by different approaches [7]. The adaptive spectrogram is defined by ([4] and [5])

$$AS(t, \omega) = 2\sum_{p=0}^{P-1} |A_p|^2 e^{-\alpha_p(t-t_p)^2 - (\omega - \omega_p - \beta_p t)^2/\alpha_p} \tag{12}$$

which is non-negative. When the residual is equal to zero, the energy contained in $AS(t,\omega)$ is the same as the signal's energy. Table 2 lists the processing time for each different method.

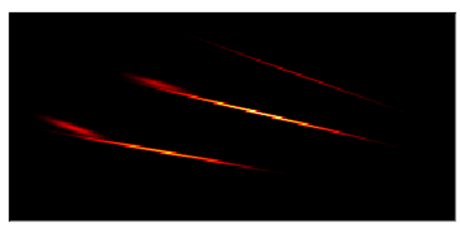

Figure 3 Chirplet based Adaptive Spectrogram (5 chirplets)

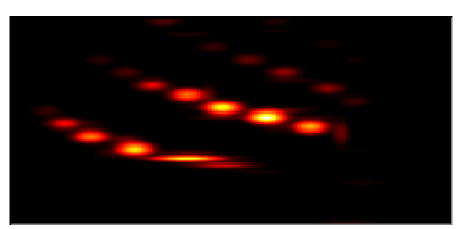

Figure 4 Frequency Modulated Gaussian Function based Adaptive Spectrogram

Compare Figure 3, the chirplet based adaptive spectrogram, and Figure 4, the frequency modulated Gaussian function based adaptive spectrogram. It is obvious that the chirplet matches the signal better. Compared to other methods, the chirplet based spectrogram not only has good time-frequency resolution, but also has a moderate computing speed.

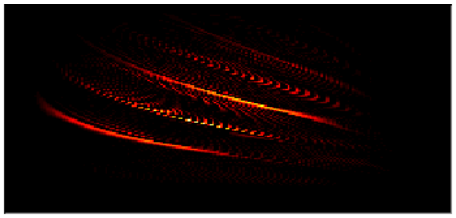

Figure 5 Pseudo Wigner-Ville Distribution

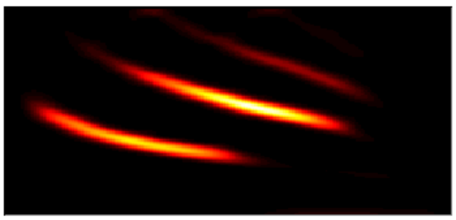

Figure 6 STFT Spectrogram

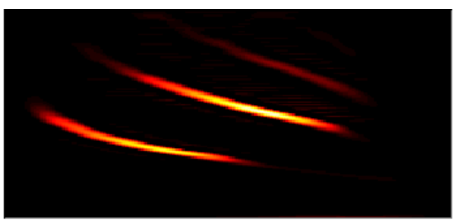

Figure 7 Gabor Spectrogram (order = 4)

Table 2:

Method	Processing Time (second)
Chirplet based Adaptive Spectrogram (5 chirplets)	0.93
Frequency modulated Gaussian based Adaptive Spectrogram	0.35
STFT Spectrogram	0.36
Pseudo Wigner-Ville Distribution	0.29
Gabor Spectrogram (order = 4)	3.13

5. SUMMARY

Using both time and frequency information, we develop an efficient algorithm for estimating optimal elementary chirplet functions. The resulting adaptive chirplet based signal approximation not only can better characterize the underlying signal than the previously known chirplet based signal's representations, but also has moderate computing speed. During extensive testing, the algorithm presented in this paper has been found to be robust and stable.

6. REFERENCES

[1] R.G. Baraniuk and D.L. Jones, "Shear madness: New orthonormal bases and frames using chirp functions," *IEEE Trans. Signal Processing*, vol.41, No.12, pp.3543-3549, December 1993.

[2] S. Mallat and Z. Zhang, "Matching pursuit with time-frequency dictionaries," *IEEE Trans. Signal Processing*, vol. 41, No.12, pp. 3397-3415, December 1993.

[3] S. Mann and S. Haykin, "The chirplet transform: Physical considerations," *IEEE Trans. Signal Processing*, vol.43, pp.2745-2461, November 1995.

[4] S. Qian, D. Chen, and K. Chen, "Signal approximation via data-adaptive normalized Gaussian functions and its applications for speech processing," *Proc. ICASSP-92*, San Francisco, CA, March 23-26, 1992, pp. 141-144.

[5] S. Qian and D. Chen, "Signal representation using adaptive normalized Gaussian functions," *Signal Processing*, vol. 36, no. 1, pp. 1-11, March 1994.

[6] S. Qian, M. E. Dunham, and M. J. Freeman, "Trans-ionospheric signal recognition by joint time-frequency representation," *Radio Science*, vol. 30, no. 6, pp. 1817-1829, November-December 1995.

[7] S. Qian and D. Chen, *Joint Time-Frequency Analysis*, Prentice-Hall, 1996.

[8] Q. Yin, Z. Ni, S. Qian, and D. Chen, "Adaptive Oriented Orthogonal Projective Decomposition," *Journal* of *Electronic* (Chinese), vol.25, No.4, pp.52-58, April 1997.